Monthly Notices of the ROYAL ASTRONOMICAL SOCIETY

MNRAS **517,** L31–L35 (2022) https://doi.org/10.1093/mnrasl/slac103
Advance Access publication 2022 September 8

Chandrasekhar-mass white dwarfs are the progenitors of a small fraction of Type Ia supernovae according to nucleosythesis constraints

Eduardo Bravo [1]★ Luciano Piersanti [2,3]★ Stéphane Blondin [4] Inma Domínguez,[5] Oscar Straniero[2,6] and Sergio Cristallo[2,3]

[1]*E.T.S. Arquitectura del Vallès, Universitat Politècnica de Catalunya, Carrer Pere Serra 1-15, E-08173 Sant Cugat del Vallès, Spain*
[2]*INAF - Osservatorio Astronomico d'Abruzzo, via Mentore Maggini, snc, I-64100, Teramo, Italy*
[3]*INFN - Sezione di Perugia, via Pascoli, Perugia I-06123, Italy*
[4]*Aix Marseille Univ, CNRS, CNES, LAM, Marseille F-13007, France*
[5]*Departamento de Física Teórica y del Cosmos, Universidad de Granada, E-18071 Granada, Spain*
[6]*INFN, Sezione di Roma, Piazzale Aldo Moro 2, I-00185 Roma, Italy*

Accepted 2022 September 3. Received 2022 August 27; in original form 2022 July 27

ABSTRACT

The precise progenitor system of type Ia supernovae (SNe Ia), whether it is a white dwarf (WD) close to the Chandrasekhar limit or substantially less massive, has been a matter of debate for decades. Recent research by our group on the accretion and simmering phases preceding the explosion of a massive WD has shown that the central density at thermal runaway lies in the range $3.6 - 6.3 \times 10^9$ g cm^{-3} for reasonable choices of accretion rate on to the WD and progenitor metallicity. In this work, we have computed one-dimensional simulations of the explosion of such WDs, with special emphasis on the chemical composition of the ejecta, which in all cases is extremely rich in neutronized isotopes of chromium (^{54}Cr) and titanium (^{50}Ti). We show that, in order to reconcile such a nucleosynthesis with the isotopic abundances of the Solar system, Chandrasekhar-mass WDs can account for at most 26 per cent of normal-luminosity SNe Ia, or at most 20 per cent of all SNe Ia.

Key words: hydrodynamics – nuclear reactions, nucleosynthesis, abundances – supernovae: general – white dwarfs – Galaxy: abundances.

1 INTRODUCTION

Although there is consensus that Type Ia supernovae (SNe Ia) are the result of the thermonuclear explosion of carbon-oxygen white dwarfs (WDs), the details of the evolutive path towards the explosion are still a subject of intense research: in particular, whether only a single WD takes part in the explosion (single degenerate, or SD, channel; Whelan & Iben 1973) or two (double degenerate, or DD, channel, Iben & Tutukov 1984; Webbink 1984), and its implications for the evolution of SNe Ia over cosmic time. Insight on the pre-eminence of one channel over the other has been provided by, e.g. the non-detection of radio and X-ray emission expected from the interaction of SNe Ia with a circumstellar medium, the absence of bloated companions that should survive thousands of years after the explosion, the search for signatures of hydrogen ablated from the companion star, the time dependence of the rate of SNe Ia explosions after a burst of star formation, or the search for a surviving binary companion close to SNe Ia remnants. A review of the theme can be found in Maoz, Mannucci & Nelemans (2014).

A related but quite different issue, more directly related to the properties of the supernova, is the structure of the WD at the time of explosion: whether the exploding object is a massive WD close to its structural instability limit, i.e. a Chandrasekhar-mass WD progenitor (Ch-m WD), or its mass is smaller than $\sim$1.2 M$_\odot$, i.e. a sub-Chandrasekhar mass WD progenitor (subCh-m WD). Ch-m WDs can explode through two different mechanisms: a pure deflagration (Nomoto 1982) or a delayed detonation (DDT; Khokhlov 1991); subCh-m WDs should detonate, and require an external trigger (detonation of an accreted He-shell or a collision/merger event; Woosley & Weaver 1994; Rosswog et al. 2009; Pakmor et al. 2012).

The quest to determine which of Ch-m or subCh-m WDs are the dominant progenitor of SNe Ia explosions has given mixed results. On the one hand, the Ch-m WD scenario is disfavoured by the failure to detect radiation associated with matter accretion on to a WD (Gilfanov & Bogdán 2010) and by the small fraction of hydrogen ionization in SNe Ia remnants (SN 1572, SN 1006, and 0509-67.5; Woods et al. 2017, 2018) and nebulae (Kuuttila et al. 2019). Flörs et al. (2020) measure the ratio of Ni II to Fe II in 58 SNe Ia and find that Ch-m WD explosions can only account for 11 per cent of their data (see also Blondin et al. 2022), and similar conclusions are reached by Eitner et al. (2020) based on the evolution of the Galactic abundance of manganese. Souropanis et al. (2022) confront predictions of nebular optical line fluxes, derived from models of accreting WDs burning hydrogen or helium on their surfaces, to observations of nebulae close to supersoft X-ray sources and SNe Ia remnants, and they are able to discriminate the models, leaving open just two possible accretion scenarios: direct C + O accretion on to a WD (slow merger of a DD leading to a Ch-m WD), and SD with accretion of He on to a subCh-m WD.

★ E-mail: eduardo.bravo@upc.edu (EB); luciano.piersanti@inaf.it (LP)

© 2022 The Author(s)
Published by Oxford University Press on behalf of Royal Astronomical Society

Downloaded from https://academic.oup.com/mnrasl/article/517/1/L31/6694255 by inaf user on 28 September 2022

Table 1. Model WDs at thermal runaway and explosion results.

Model	$Z_{\rm ini}$ (10^{-3})	$\dot{M}_{\rm acc}$ ($M_\odot$ yr^{-1})	$\rho_{T\rm max}$ (g cm^{-3})	$E_{\rm kin}$ (foes)	M_{56} ($M_\odot$)
Z14	0.245	10^{-7}	5.02×10^9	1.318	0.656
Z63	6.000	10^{-7}	5.28×10^9	1.300	0.642
Z12	13.80	10^{-7}	5.41×10^9	1.294	0.619
Z22	20.00	10^{-7}	5.56×10^9	1.281	0.595
Z42	40.00	10^{-7}	6.34×10^9	1.263	0.553
R2m7	13.80	2×10^{-7}	5.03×10^9	1.306	0.615
R6m7	13.80	6×10^{-7}	3.67×10^9	1.325	0.640
R9m7	13.80	9×10^{-7}	3.69×10^9	1.309	0.615

Note. 1 foe $= 10^{51}$ ergs

On the other hand, the subCh-m WD scenario is subdominant according to analyses of the abundances in the intra-cluster medium (Mernier et al. 2016), and Scalzo, Ruiter & Sim (2014) and Scalzo et al. (2019) estimate about the same number of Ch-m and subCh-m WDs from their analysis of the light curves of several hundred SNe Ia. Moreover, detailed studies of the evolution of AM CVn systems with either a He star or a He WD accreting on to a C-O WD show no clear path towards a thermonuclear explosion that might give birth to SNe Ia (Brooks et al. 2015; Piersanti, Yungelson & Tornambé 2015; Piersanti et al. 2019). Here, we present new evidence of a small contribution of Ch-m WD to SNe Ia, on the basis of pre-supernova evolution calculations followed by explosion models.

Until now, the lack of detailed Ch-m WD evolutionary models up to the time of thermal runaway has left the ignition density largely uncertain. Simulations of the explosion and chemical evolution calculations have assumed a given central density at thermal runaway ($\rho_{\rm c}$) or they have explored the effects of different densities, often exploiting the freedom to mix results from different $\rho_{\rm c}$. In Piersanti et al. (2022, hereafter Paper I), we revisited the pre-explosive evolution of accreting WDs up to the onset of thermal runaway including the best available treatments of the physical processes believed to play a relevant role (a list of prior works on the simmering phase can be found in Paper I). A key result of the new simmering calculations is that *ρ_c is very high in all exploding Ch-m WDs: $\rho_c > 3.6 \times 10^9$* g cm^{-3}.

In this letter, we follow the evolution through the explosive phase of the runaway WDs computed in Paper I. In the following sections, we describe our methods and results, and quantify the limits posed by the nucleosynthesis to the contribution of Ch-m WDs to SNe Ia. Our results imply that the Ch-m WD scenario cannot have been dominant among the SNe Ia that contributed to the chemical enrichment of the Solar system neighbourhood. Finally, we discuss the limits of our approach and give our conclusions.

2 MASSIVE WD EXPLOSIONS

In Paper I, we show that accounting for the URCA processes associated with the most abundant species is crucial to accurately determine the structure of Ch-m WDs on the verge of explosion. In particular, the molecular weight gradient at the URCA shells confines convection to a small volume near the centre, in sharp contrast to previous belief that convection encompasses up to $\sim$1 $M_\odot$ of the WD. In Table 1, we give the main properties of the computed Ch-m WDs at thermal runaway (we adopt the model name convention of Paper I): the progenitor metallicity, $Z_{\rm ini}$, the accretion rate on to the exploding WD, $\dot{M}_{\rm acc}$, and the density of the hottest shell at thermal runaway, $\rho_{T\rm max}$, ranging from a minimum of 3.6×10^9 g cm^{-3} up to more than 6×10^9 g cm^{-3}. The minimum $\rho_{T\rm max}$ is obtained for high accretion rates, $\dot{M}_{\rm acc} \gtrsim 5 \times 10^{-7}$ $M_\odot$ yr^{-1}.

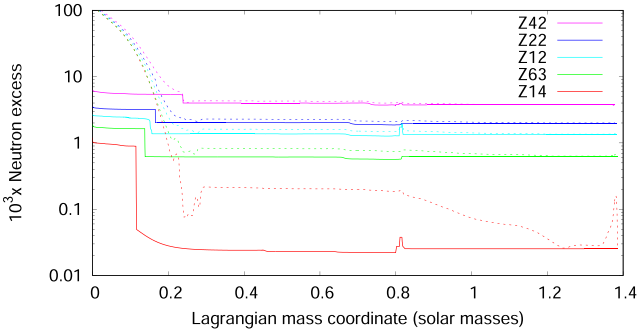

Figure 1. Profile of neutron excess, $\eta = \Sigma(N_i - Z_i)\ Y_i$ (where Y_i is the molar fraction of species i) at the end of the simmering phase (solid lines) and 2,000 s after thermal runaway (dotted lines) for the models with different progenitor metallicity (Z42, Z22, Z12, Z63, and Z14, from top to bottom). The high final neutron excess in model Z14 beyond $M \sim 0.25\,M_\odot$ is due to the decay of short-lived radioactive isotopes during the early post-explosion phase.

As it is well known, the outcome of the explosion of a massive WD is not uniquely determined by the initial conditions, at least not in a way that we understand well enough. We have selected delayed DDT as the explosion mechanism, characterized by two parameters: a constant flame velocity (in terms of the sound speed) during the deflagration epoch, $v_{\rm def}/v_{\rm sound} = 0.03$, and a transition density from deflagration to detonation, $\rho_{\rm DDT} = 2.4 \times 10^7$ g cm^{-3}. This setup has proven in past simulations to provide spectra and light curves compatible with the observed properties of normal SNe Ia (e.g. Blondin et al. 2013, although their $\rho_{\rm c}$ is lower than ours). The one-dimensional hydrodynamic code used in the present calculations is described in Bravo, Badenes & Martínez-Rodríguez (2019).

Table 1 shows the final kinetic energy, $E_{\rm kin}$, and the ejected mass of ^{56}Ni, M_{56}. The latter lies in the range $0.60 \pm 0.05\,M_\odot$, close to the value obtained by Blondin et al. (2013) for their model DDC10, which is a close match to SN 2005cf, considered a 'golden standard' for typical SNe Ia. The kinetic energy is almost the same in all models in Table 1, but substantially smaller than the kinetic energy of model DDC10, likely due to the higher binding energy of the initial WD in the present models (DDC10 starts from a $\rho_{\rm c}$ of 2.6×10^9 g cm^{-3}). The ejected (final, after radioactive decays) iron mass of the models in Table 1 is in the range $0.75 \pm 0.01\,M_\odot$, and the ratio of chromium mass to iron mass is on the order of 0.03 in all models, about twice the Solar system ratio. However, these two elements are quite differently distributed through the ejecta: while chromium is mainly produced during the initial deflagration and concentrated in the most internal portion of the ejecta, iron is more or less evenly distributed along the deflagrated and detonated zones. Other iron-peak elements (titanium, manganese, and nickel) are underproduced or overproduced with respect to iron depending on the progenitor metallicity. Notably, different WD accretion rates produce almost identical chemical profiles, similar to model DDC10 and are expected to lead to indistinguishable optical outputs.

The profile of the neutron excess, η, 2,000 s after thermal runaway is shown in Fig. 1, together with the neutron excess at the end of the simmering phase. Two quite different regions can be identified in all the η profiles. Below a mass coordinate of $\sim$0.2 $M_\odot$, the neutron excess is quite large and almost independent of the details of the initial WD structure. This behaviour is a result of the high electron capture rate in nuclear statistical equilibrium at the high densities

Downloaded from https://academic.oup.com/mnrasl/article/517/1/L31/6694255 by inaf user on 28 September 2022

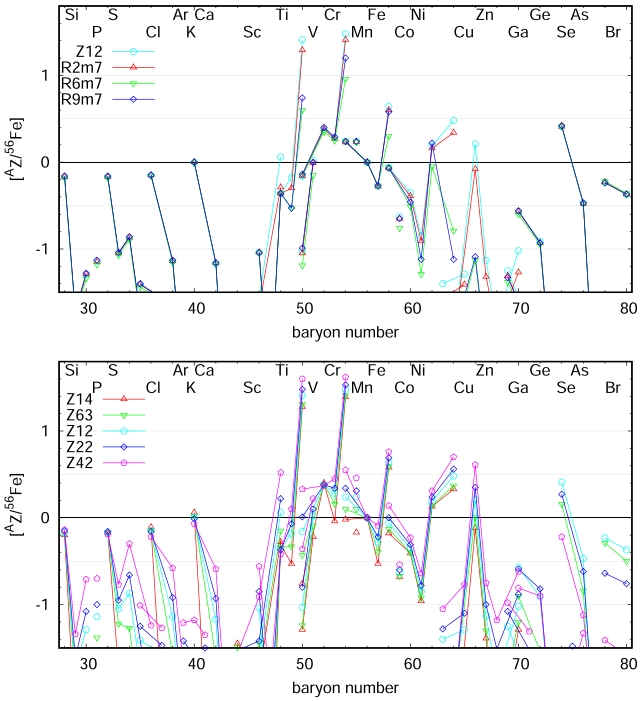

Figure 2. Final composition after radioactive decays for the models with different $\dot{M}_{\rm acc}$ (top) and $Z_{\rm ini}$ (bottom): $\left[{}^{A}Z/{}^{56}{\rm Fe}\right] = \log_{10}\left[m\left({}^{A}Z\right)/m\left({}^{56}{\rm Fe}\right)\right] - \log_{10}\left[m\left({}^{A}Z\right)/m\left({}^{56}{\rm Fe}\right)\right]_{\odot}$..

that characterize all models during the initial deflagrative phase. There, the electron capture rate is so high that all memory of the initial neutron excess is erased. Above the aforementioned mass coordinate, matter is burnt at a density small enough that there are negligible amounts of electron captures during the explosion and, consequently, the neutron excess reflects the initial metallicity of the progenitor WD.

The chemical composition of the ejecta is shown in Fig. 2. The first thing to note is that the composition is almost completely independent of the accretion rate on to the WD. There are, however, a few neutron-rich species that are more sensitive to the different central densities derived from the simmering evolution under different accretion rates. In all models, the most overproduced species (with respect to the reference, ^{56}Fe and the Solar system composition) are ^{54}Cr and ^{50}Ti, with production factors above nine, even for small accretion rates. Among all the different progenitor metallicities, $Z = 2.45 \times 10^{-4}$ produces the least amount of ^{54}Cr, but its production factor is still on the order of 25. All the ^{54}Cr is produced in the region with $\eta \simeq 0.1$, close to the centre (see Fig. 1). Thus, our simmering + explosion calculations show that *all SNe Ia coming from Ch-m WDs are characterized by a large overproduction of* ^{54}*Cr and* ^{50}*Ti*. Indeed, high Cr/Fe ratios have been found in the SNe Ia remnant 3C 397 (Yamaguchi et al. 2015; Ohshiro et al. 2021), and measurements of the isotopic composition of some meteoritic grains show correlated enrichments of ^{54}Cr and ^{50}Ti (Nittler et al. 2018), in agreement with our nucleosynthetic results.

3 CONTRIBUTION OF CH-M WDS TO SNE IA

The overproductions of ^{54}Cr and ^{50}Ti in our models limit the fraction of SNe Ia that can result from Ch-m WD explosions. Even in our most favourable case, model R6m7, and assuming that Ch-m SNe Ia are the only source of ^{54}Cr, only a few explosions of these massive WDs would be allowed to pollute the solar neighbourhood in order to reproduce the Solar system abundances.

In this section, we quantify upper limits to the *fraction of normal SNe Ia* that can be produced by the thermonuclear explosion of *Chandrasekhar-mass WDs*, which we represent with $X_{\rm Ch}^{\rm nor}$. First, we define: $M_{\rm Fe}$, the total mass of Fe in the solar neighbourhood; M_{54}, the total mass of ^{54}Cr in the solar neighbourhood; $f_{\rm Fe,\,Ia}$, the fraction of the Fe mass due to SNe Ia; $X_{\rm sl}$, the fraction by number of subluminous SNe Ia over the total number of SNe Ia; $m_{\rm Fe}^{\rm nor}$, the mean mass of Fe ejected in a normal SNe Ia, for both Ch-m and SubCh-m progenitors; $m_{\rm Fe}^{\rm sl}$, the mass of Fe ejected in a subluminous SNe Ia; $m_{54}^{\rm Ch}$, the mass of ^{54}Cr ejected in a Ch-m WD SNe Ia; and $N_{\rm Ia}$, the total number of SNe Ia events in the solar neighbourhood. To start, we assume that Ch-m WDs do not contribute to sub-luminous SNe Ia, and that neither core-collapse SNe nor SNe Ia from subCh-m WDs synthesize any ^{54}Cr (in order to maximize the upper limits to $X_{\rm Ch}^{\rm nor}$). Then,

$$M_{\rm Fe} = N_{\rm Ia}\left[X_{\rm sl} m_{\rm Fe}^{\rm sl} + (1 - X_{\rm sl})\, m_{\rm Fe}^{\rm nor}\right] / f_{\rm Fe,Ia}, \quad (1)$$

and

$$M_{54} = N_{\rm Ia} X_{\rm Ch}^{\rm nor} (1 - X_{\rm sl})\, m_{54}^{\rm Ch}. \quad (2)$$

Next, we constrain the ratio of the total masses of Fe and ^{54}Cr to match with the correspondent Solar system ratio: $M_{54}/M_{\rm Fe} = (M_{54}/M_{\rm Fe})_{\odot}$, and we assign reasonable values to some of the above parameters: $m_{\rm Fe}^{\rm nor} = 0.75\,{\rm M}_{\odot}$, $m_{\rm Fe}^{\rm sl} = 0.25\,{\rm M}_{\odot}$, $X_{\rm sl} = 0.20$ (Li et al. 2011). Normal SNe Ia are expected to eject an iron mass in the range $\sim$0.4–0.95 $\rm M_{\odot}$, with a mean close to the value we adopt for $m_{\rm Fe}^{\rm nor}$. Although the parameter $f_{\rm Fe,\,Ia}$ is not tightly constrained, we adopt here the range from 50 per cent to 67 per cent, based on chemical evolution arguments (Timmes, Woosley & Weaver 1995; Prantzos et al. 2018). Another way to determine $f_{\rm Fe,\,Ia}$ is through the rates of different types of SNe, around one SNe Ia every 3-4 core-collapse events (Li et al. 2011; Kubryk, Prantzos & Athanassoula 2015; Prantzos et al. 2018), combined with their iron yields, about ten times larger in SNe Ia than in core-collapse SNe, with the result that the contribution of SNe Ia to the iron mass could be as much as 75 per cent. Therefore, our adopted range for $f_{\rm Fe,\,Ia}$ is quite conservative. Finally,

$$X_{\rm Ch}^{\rm nor} = \frac{1 - X_{\rm sl}\left(1 - m_{\rm Fe}^{\rm sl}/m_{\rm Fe}^{\rm nor}\right)}{(1 - X_{\rm sl})\, f_{\rm Fe,Ia}{\rm pf}(^{54}{\rm Cr})}, \quad (3)$$

where ${\rm pf}(^{54}{\rm Cr}) = \frac{m_{54}^{\rm Ch}/m_{\rm Fe}^{\rm nor}}{(M_{54}/M_{\rm Fe})_{\odot}}$ is the production factor of ^{54}Cr in normal-luminosity Ch-m WDs. We remark that, in order to maintain compatibility with the constraints on the contribution of SNe Ia to the chemical enrichment of the ISM, we define the production factor of ^{54}Cr with respect to element iron instead of ^{56}Fe, as is common practice. In the present models, pf(^{54}Cr) goes from 8.4, for model R6m7, to 33.8, for model Z42. Applying equation (3), the predicted fraction of Ch-m WDs among normal SNe Ia goes from 5 per cent and up to a maximum of 26 per cent.

One can easily relax the assumption that the fraction of Ch-m WDs among sub-luminous SNe Ia , $X_{\rm Ch}^{\rm sl}$, is different from zero. Since ^{54}Cr is synthesized during the first second of the deflagration phase, which is common to all the explosion mechanisms of Ch-m WDs currently considered (e.g. Woosley 1997), we assume that the yield of ^{54}Cr in sub-luminous SNe Ia from Ch-m WDs is the same as in their normal luminosity counterparts, $m_{54}^{\rm Ch}$. Then, the production factor of ^{54}Cr in sub-luminous SNe Ia from Ch-m WDs is three times larger than in normal SNe Ia from the same mass range. In this case, equation (3) is replaced by a monotonouly decreasing linear relationship between $X_{\rm Ch}^{\rm nor}$ and $X_{\rm Ch}^{\rm sl}$, shown in Fig. 3. In the most optimistic case, $X_{\rm Ch}^{\rm nor}$ decreases from a maximum of 26 per cent, for

Downloaded from https://academic.oup.com/mnrasl/article/517/1/L31/6694255 by inaf user on 28 September 2022

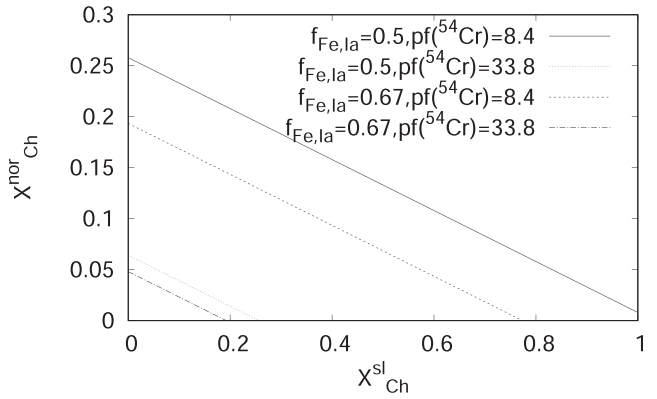

Figure 3. The fraction of normal SNe Ia originating from Chandrasekhar-mass WDs, X^{nor}_{Ch}, as a function of the fraction of sub-luminous SNe Ia that result from the explosion of Chandrasekhar-mass WDs, X^{sl}_{Ch}, for four combination of parameters $f_{Fe,\,Ia}$ and pf(^{54}Cr).

$X^{sl}_{Ch} = 0$, to a negligible value when $X^{sl}_{Ch} = 1$, i.e. with the current uncertainties in the production factor of ^{54}Cr and in $f_{Fe,\,Ia}$, Ch-m WDs could account for all sub-luminous SNe Ia , although at the cost of not contributing to normal SNe Ia. Whatever the value of X^{sl}_{Ch}, the fraction of all SNe Ia due to Ch-m WD explosions is limited to less than 20 per cent.

4 DISCUSSION

The stellar evolution calculations presented in Paper I include all the physical processes relevant to the pre-explosive WD evolution. Nevertheless, there are a few aspects that cannot or still have not been incorporated in the one-dimensional hydrostatic code, in particular rotation and magnetism, whose potential role in the simmering phase is hard to predict. Another improvement would be the modelling of the last minutes of the pre-explosive phase in three dimensions (e.g. Nonaka et al. 2012), but the complexity of such a task makes it difficult to incorporate the level of physical detail that we have found relevant to the simmering phase.

The explosive nucleosynthesis might be sensitive to both nuclear reaction uncertainties and to multidimensional hydrodynamical processes. However, the yield of ^{54}Cr is almost insensitive to nuclear reaction and electron capture rates (Bravo & Martínez-Pinedo 2012; Bravo 2019). On the other hand, a strong buoyancy of hot ash bubbles might reduce the time that incinerated matter stay at high density and decrease the amount of electron captures, hence decreasing the yield of neutron-rich nuclei such as ^{54}Cr and ^{50}Ti. However, the high electron capture rates at the central densities of our models translate into an increase in density of the hot bubbles in order to keep pressure constant during the almost isobaric deflagration phase, which, in turn, impacts their buoyancy. In order to estimate the last effect, we have followed the methods in Fisher & Jumper (2015, Appendix A) and Bravo (2019, Section 3). We find that, at densities above 5.5×10^9 g cm^{-3}, the bubbles are not able to float to the surface of the WD but, instead, they turn towards the centre after a time ∼0.9 s. At slightly lower densities, $4 \times 10^9 \lesssim \rho \lesssim 5.5 \times 10^9$ g cm^{-3}, the rising of the bubbles is delayed nearly one second as compared with their evolution without electron captures. Such a delay is long enough to allow the synthesis of a large mass of ^{54}Cr and ^{50}Ti.

Indeed, there are a few multidimensional simulations of SNe Ia starting from high-ρ_c WDs and based on the DDT mechanism, and they find a large overproduction of ^{54}Cr, in line with our results. Seitenzahl et al. (2013) explode a WD with a ρ_c of 5.5×10^9 g cm^{-3} and synthesize 0.69 $M_\odot$ of ^{56}Ni (model N100H). Their production factor of ^{54}Cr with respect to ^{56}Fe is five. As could be expected, the setup of model N100H is not completely consistent with our simmering models. The geometry of the initially burnt region in N100H consists of 100 spherical ignition kernels of 10 km radius distributed through a central sphere of radius 150 km, which is beyond the maximum extension of the convective core in several of our simmering models. Besides, in N100H, the initial chemical composition of the WD is 50 per cent-50 per cent carbon and oxygen, again at odds with the carbon-abundance profiles presented in Paper I. Dave et al. (2017) computed a high ρ_c model in two dimensions, starting from a single igniting bubble of 100 km size located at the centre of a WD with a ρ_c of 6×10^9 g cm^{-3}. This model overproduces ^{54}Cr by a factor ∼50. Besides the different dimensionality of the calculation, Dave et al. (2017) assume an initially uniform chemical composition made of 30 per cent carbon and 70 per cent oxygen, close to the values of our simmering models. Leung & Nomoto (2018) compute several two-dimensional DDT models with a ρ_c of 5×10^9 g cm^{-3}, with ^{54}Cr overproductions ranging from 17 to 22.

With respect to the gravitationally confined detonation mechanism (GCD), it is based on the fast rise of a hot incinerated bubble burnt near the centre to the surface of the WD (Plewa, Calder & Lamb 2004). Since we have shown that the rising of hot ash bubbles is, at the best, strongly delayed by electron captures at high ρ_c, we conclude that Chandrasekhar-mass WDs are not prone to explode following the GCD paradigm.

5 CONCLUSIONS

Our hydrodynamic explosion models of SNe Ia are extremely rich in the neutronized species ^{54}Cr and ^{50}Ti, a result that follows directly from the high ρ_c found in previous pre-explosive simmering calculations (Paper I). It is important to note that these simmering calculations leave no room for Ch-m WD explosions at ρ_c below 3.5×10^9 g cm^{-3}. Thus, we can discard approaches in which the nucleosynthesis of high-ρ_c SNe Ia can be partly compensated by considering a fraction of low-ρ_c explosions, e.g. at $\sim 2 \times 10^9$ g cm^{-3}.

In particular, the overproduction of ^{54}Cr in our SNe Ia models ranges from 8 (for fast accretion rates) to 34 (for slow accretion rates and super-solar metallicity). Using these overproduction factors of ^{54}Cr together with reasonable guesses for the contribution of SNe Ia to the total mass of iron in the solar neighbourhood and for the fraction of sub-luminous SNe Ia, we derive an upper limit of 5 − 26 per cent to the fraction of normal SNe Ia that can originate from the explosion of Ch-m WDs. The fraction of Ch-m WD progenitors over the total number of SNe Ia is found to be smaller than 20 per cent, even when allowing for a contribution of high-density Ch-m WDs to the sub-luminous sample of SNe Ia.

ACKNOWLEDGEMENTS

We thank Dr. Leung for email exchange concerning published yields. EB thanks Amador Alvarez, Esther Nadal and the rest of the staff of CCLAIA of ETSAV for their continued support. This publication is part of the projects I + D + I PGC2018-095317-B-C21 funded by MICINN/AEI/10.13039/501100011033 and FEDER 'A way of doing Europe' (EB and ID), and PID2021-123110NB-I00 (ID). LP and OS acknowledge financial support from the INAF - mainstream project 'Type Ia Supernovae Parent Galaxies: Expected Results from LSST', and their participation to the VANS project on 'Standard candles in astrophysics: Atomic and Nuclear physics in SNIa', which

Downloaded from https://academic.oup.com/mnrasl/article/517/1/L31/6694255 by inaf user on 28 September 2022

was funded by the University of Campania Luigi Vanvitelli (Italy). This work was supported by the 'Programme National de Physique Stellaire' (PNPS) of CNRS/INSU co-funded by CEA and CNES (SB). SB acknowledges support from the ESO Scientific Visitor Programme in Garching.

DATA AVAILABILITY

The data underlying this article will be shared on reasonable request to the corresponding author.

REFERENCES

Blondin S., Dessart L., Hillier D. J., Khokhlov A. M., 2013, MNRAS, 429, 2127
Blondin S., Bravo E., Timmes F. X., Dessart L., Hillier D. J., 2022, A&A, 660, A96
Bravo E., 2019, A&A, 624, A139
Bravo E., Martínez-Pinedo G., 2012, Phys. Rev. C, 85, 055805
Bravo E., Badenes C., Martínez-Rodríguez H., 2019, MNRAS, 482, 4346
Brooks J., Bildsten L., Marchant P., Paxton B., 2015, ApJ, 807, 74
Dave P., Kashyap R., Fisher R., Timmes F., Townsley D., Byrohl C., 2017, ApJ, 841, 58
Eitner P., Bergemann M., Hansen C. J., Cescutti G., Seitenzahl I. R., Larsen S., Plez B., 2020, A&A, 635, A38
Fisher R., Jumper K., 2015, ApJ, 805, 150
Flörs A. et al., 2020, MNRAS, 491, 2902
Gilfanov M., Bogdán Á., 2010, Nature, 463, 924
Iben I. Jr, Tutukov A. V., 1984, ApJS, 54, 335
Khokhlov A. M., 1991, A&A, 245, 114
Kubryk M., Prantzos N., Athanassoula E., 2015, A&A, 580, A126
Kuuttila J., Gilfanov M., Seitenzahl I. R., Woods T. E., Vogt F. P. A., 2019, MNRAS, 484, 1317
Leung S.-C., Nomoto K., 2018, ApJ, 861, 143
Li W. et al., 2011, MNRAS, 412, 1441
Maoz D., Mannucci F., Nelemans G., 2014, ARA&A, 52, 107
Mernier F. et al., 2016, A&A, 595, A126
Nittler L. R., Alexander C. M. O., Liu N., Wang J., 2018, ApJ, 856, L24
Nomoto K., 1982, ApJ, 253, 798
Nonaka A., Aspden A. J., Zingale M., Almgren A. S., Bell J. B., Woosley S. E., 2012, ApJ, 745, 73
Ohshiro Y. et al., 2021, ApJ, 913, L34
Pakmor R., Kromer M., Taubenberger S., Sim S. A., Röpke F. K., Hillebrandt W., 2012, ApJ, 747, L10
Piersanti L., Yungelson L. R., Tornambé A., 2015, MNRAS, 452, 2897
Piersanti L., Yungelson L. R., Cristallo S., Tornambé A., 2019, MNRAS, 484, 950
Piersanti L., Bravo E., Straniero O., Cristallo S., Domínguez I., 2022, ApJ, 926, 103 (Paper I)
Plewa T., Calder A. C., Lamb D. Q., 2004, ApJ, 612, L37
Prantzos N., Abia C., Limongi M., Chieffi A., Cristallo S., 2018, MNRAS, 476, 3432
Rosswog S., Kasen D., Guillochon J., Ramirez-Ruiz E., 2009, ApJ, 705, L128
Scalzo R. A., Ruiter A. J., Sim S. A., 2014, MNRAS, 445, 2535
Scalzo R. A. et al., 2019, MNRAS, 483, 628
Seitenzahl I. R. et al., 2013, MNRAS, 429, 1156
Souropanis D., Chiotellis A., Boumis P., Chatzikos M., Akras S., Piersanti L., Ruiter A. J., Ferland G. J., 2022, MNRAS, 513, 2369
Timmes F. X., Woosley S. E., Weaver T. A., 1995, ApJS, 98, 617
Webbink R. F., 1984, ApJ, 277, 355
Whelan J., Iben Icko J., 1973, ApJ, 186, 1007
Woods T. E., Ghavamian P., Badenes C., Gilfanov M., 2017, Nature Astron., 1, 800
Woods T. E., Ghavamian P., Badenes C., Gilfanov M., 2018, ApJ, 863, 120
Woosley S. E., 1997, ApJ, 476, 801
Woosley S. E., Weaver T. A., 1994, ApJ, 423, 371
Yamaguchi H. et al., 2015, ApJ, 801, L31

This paper has been typeset from a TEX/LATEX file prepared by the author.

Downloaded from https://academic.oup.com/mnrasl/article/517/1/L31/6694255 by inaf user on 28 September 2022